Cement & Concrete Composites 34 (2012) 156–165

Contents lists available at SciVerse ScienceDirect

Cement & Concrete Composites

journal homepage: www.elsevier.com/locate/cemconcomp

Frost resistance and microstructure of Engineered Cementitious Composites: Influence of fly ash and micro poly-vinyl-alcohol fiber

Mustafa Şahmaran [a,*], Erdoğan Özbay [b], Hasan E. Yücel [a], Mohamed Lachemi [c], Victor C. Li [d]

[a] Department of Civil Engineering, Gaziantep University, Gaziantep, Turkey
[b] Department of Civil Engineering, Mustafa Kemal University, Antakya, Turkey
[c] Department of Civil Engineering, Ryerson University, Toronto, ON, Canada
[d] Department of Civil and Environmental Engineering, University of Michigan, Ann Arbor, MI, United States

ARTICLE INFO

Article history:
Received 8 October 2010
Received in revised form 30 September 2011
Accepted 1 October 2011
Available online 8 October 2011

Keywords:
Engineered Cementitious Composites (ECC)
Frost resistance
Fly ash
PVA fibers
Microstructure

ABSTRACT

One of the most damaging environmental conditions to concrete structure is cyclic freezing and thawing. This paper discusses the influence of the high volumes of fly ash (FA) and micro poly-vinyl-alcohol (PVA) fibers on the cyclic freeze–thaw resistance and microstructure of the Engineered Cementitious Composites (ECC). ECC mixtures with two different FA–cement (FA/C) ratios (1.2 and 2.2 by weight), and at constant water-cementitious materials (fly ash and cement) ratio of 0.27 are prepared. To compare the behavior of ECC with ECC matrix, all of the preceding properties are also investigated for ECC matrix mixtures of same composition without PVA fiber. For frost resistance, mixtures are exposed to the freeze and thaw cycles up to 300 cycles in accordance with ASTM C666, Procedure A. Experimental tests consist of measuring the residual mechanical properties (flexural strength, mid-span beam deflection and flexural stress – deflection curve), ultrasonic pulse velocity and mass loss. The roles of PVA fibers and FA are discussed through the analysis of microstructure and fiber–matrix interactions as function of frost exposure. The microstructural characterization by measuring pore size distributions is examined before and after exposure to frost deterioration by using mercury intrusion porosimetry (MIP). The air-void characteristics of mixtures are also studied using linear transverse method. Test results confirm that both ECC mixtures with high volumes of FA remain durable, and show a tensile strain capacity of more than 2% even after 300 freezing and thawing cycles. On the other hand, before completing 300 freezing and thawing cycles, matrix (ECC without fiber) specimens have severely deteriorated, requiring removal from the freeze–thaw machine. Therefore, results indicate that the addition of micro PVA fiber to the ECC matrix substantially improved the frost resistance. The results of freeze–thaw tests also indicated that the reduction of residual physical and mechanical properties with increasing number of freeze–thaw cycles is relatively more for ECC mixture with FA/C ratio of 2.2 than for ECC mixture with FA/C ratio of 1.2.

1. Introduction

In recent years, the effort to modify the brittle nature of ordinary concrete has resulted in modern concepts of high performance fiber reinforced cementitious composites, which are characterized by tensile strain-hardening after first cracking. Depending on its composition, its tensile strain capacity can be up to several hundred times those of normal and fiber reinforced concrete. Engineered Cementitious Composites (ECC), designed to strain harden in tension based on micromechanical principles, allows optimization of the composite for high performance represented by extreme ductility while minimizing the amount of reinforcing fibers, typically less than 2% by volume [1–3]. The most distinctive characteristic separating ECC from conventional concrete and fiber reinforced concrete (FRC) is an ultimate tensile strain capacity between 3% and 5%, depending on the specific ECC mixture. Along with tensile ductility, the unique crack development within ECC is critical to its durability. Different from ordinary concrete and most fiber reinforced concretes, ECC exhibits self-controlled crack widths under increasing load. Even at large imposed deformation, crack widths of ECC remain small, less than 60 μm. With intrinsically tight crack width and high tensile ductility, ECC represents a new concrete material that offers a significant potential to naturally resolving the durability problem of concrete structures. For these reasons, the use of ECC has become increasingly popular for the last decade, and it has been used in North America, Europe and Asia for high-rise buildings, bridges, tunnels, highways, offshore structures and other forms of infrastructures [4].

The use of concrete containing high volumes of fly ash (FA) has recently gained popularity as a resource efficient, durable, and

* Corresponding author. Tel.: +90 342 317 2410; fax: +90 342 360 1107.
E-mail address: sahmaran@gantep.edu.tr (M. Şahmaran).

0958-9465/$ - see front matter © 2011 Elsevier Ltd. All rights reserved.
doi:10.1016/j.cemconcomp.2011.10.002

sustainable option for a variety of concrete applications. Recently, FA has also become what some consider a necessary component of ECC. It is used in ECC production in replacements of up to 85% (FA/cement ratio of up to 6.5) by mass of the total cementitious material [5–7]. In addition to well known benefits of FA for concrete listed above, the addition of FA alters the microstructure of ECC; this change improves the robustness of tensile ductility while retaining a long-term tensile strain of approximately 3% [5–7] and reduces the residual crack width from about 60 μm level to 10–30 μm level or sometimes even lower than 10 μm level, but its effect on the durability of the composite is not fully known.

An increasing problem world-wide is the maintenance and rehabilitation of the infrastructure. Deterioration is accelerated in cold weather environment as the concrete is subjected to freezing and thawing cycles, one of the major causes of the rapid degradation of highway pavements, airport pavements, bridge decks and parking structures in cold climate regions. ECC used for this kind of structures must be resistant to cyclical freezing and thawing. It is known that a proper air-void system is generally needed in normal concrete to avoid internal cracking due to freeze–thaw cycles. Although the field performance of ECC generally indicates that it has a good frost resistance [8], little quantitative data has been published in the scientific and technical literature on the frost durability properties of standard ECC mixture (known also as ECC M45 that has a FA – Portland cement ratio of 1.2 [9,10]). Moreover, no research work so far has been reported on the frost durability of high volume FA (HVFA) ECC with tighter crack width. With the current extensive use of FA in ECC production and the rise in frost deterioration occurrences in recent years, a thorough understanding of the influence of FA on frost durability of ECC is urgently needed. Recent work by Şahmaran et al. on standard ECC mixture suggests that frost resistance is improved by the incorporation of PVA fiber into the mix due to the higher crack resistance and larger pore volume, and resulting pressure-releasing effects under freeze–thaw conditions, but there is little explanation given of the mechanism involved [10].

The objective of this research is to assess the effect of FA and micro-PVA fiber on the frost resistance of non-air-entrained ECC. ECC mixtures with two different FA to cement (FA/C) ratios (1.2 and 2.2) were prepared. To determine the effect of micro-fibers and ultra-high ductility of ECC, ECC matrix mixtures of the same composition but without PVA fibers were also produced and tested for the frost resistance. To evaluate the freeze–thaw durability of ECC and ECC matrix mixtures, freezing and thawing test in accordance with ASTM C666 Procedure A was conducted. The loss of mass, pulse velocity and the flexural parameters (flexural strength, mid-span beam deflection and flexural stress – deflection curve) of specimens subjected to freezing and thawing cycles are determined. In addition, air void parameters in accordance with ASTM C457 modified point count method were studied. The role of PVA fibers and FA was analyzed in terms of microstructure and fiber–matrix interactions as a function of frost exposure by using mercury intrusion porosimetry analysis.

2. Experimental studies

2.1. Materials, mixture proportions and basic mechanical properties

The materials used in the production of ECC mixtures were Type-I Portland cement (C), Class-F fly ash (FA) with a lime content of 5.6%, micro silica sand with a maximum grain size of 250 μm, water, poly-vinyl-alcohol (PVA) fibers, and a polycarboxylic-ether type high-range water reducing admixture (HRWR). Chemical composition and physical properties of portland cement and FA are presented in Table 1. The PVA fibers with a diameter of 39 μm and a length of 8 mm are purposely manufactured with a tensile strength of 1620 MPa, elastic modulus of 42.8 GPa, maximum elongation of 6.0% for ECC [3]. The PVA fiber tends to rupture instead of pull out in a cementitious matrix, as a result of the strong chemical bonding with cement due to the presence of the hydroxyl group in its molecular chains [3]. For this reason, the surface of the PVA fibers is coated with a proprietary hydrophobic oiling agent of 1.2% by mass to tailor the interfacial properties between fiber and matrix for ECC strain-hardening performance.

ECC mixtures with fly ash-cement ratio (FA/C) of 1.2 and 2.2 by mass were used in this investigation, details of which are given in Table 2. To analyze the influence of micro fibers and high tensile strain capacity on the frost resistance of ECC, matrix mixtures (ECC without PVA fibers) were also studied. All mixtures were prepared in a standard mortar mixer at a constant amount of cementitious material and constant water to cementitious material (W/CM) ratio of 0.27. HRWR was added to the mixture until the desired fresh ECC characteristics, described in another study [11], were visually observed. All ECC and ECC matrix materials used in this study contain no air-entraining admixture.

Tables 2 and 3 show compressive strength test results of the ECC and ECC matrix mixtures and the tensile behavior of ECC mixtures cured in an environmental chamber at a temperature of 23 ± 2 °C and a relative humidity of 95 ± 5% until the age of testing, respectively. The compressive strength was computed as an average of three 50 mm cubic specimens. As seen from Table 2 and as expected, the compressive strength of ECC decreased with increasing FA content and was not influenced with the incorporation of fiber to ECC matrix mixtures. Even at almost 70% replacement of portland cement with FA (FA/C = 2.2), the compressive strength of ECC at 28 days can be more than 50 MPa.

To characterize the direct tensile behavior of the ECC mixtures, 200 × 75 × 13 mm coupon specimens were used. Direct tensile tests were conducted under displacement control at a loading rate of 0.005 mm/s. The typical tensile stress–strain curves of the ECC mixtures at 14 and 28 days are shown in Fig. 1. Two specimens were tested for each mix and for each age. As seen from Table 3, the ECC composites exhibited a strain capacity of more than 2.7% at 28 days. The strain capacity measured at 28 days of age is slightly lower than the 14-day strain capacity (Fig. 1 and Table 3) but remains significantly higher than that of normal concrete. Previous studies demonstrated that the tensile strain capacity seems to stabilize after 28 days [7]. As can be seen from Table 3, the increase of FA/C ratio improves the tensile strain capacity of ECC at all ages. The improvement in the tensile strain capacity with the increase in the FA content can be attributed to the fact that increase in the FA content tends to reduce the PVA fiber/matrix interface chemical bond and matrix toughness, while increasing the interface frictional bond, in favor of attaining high tensile strain

Table 1
Properties of cement and fly ash.

Chemical composition (%)	Cement	Fly ash
CaO	61.80	5.57
SiO_2	19.40	59.50
Al_2O_3	5.30	22.20
Fe_2O_3	2.30	3.90
MgO	0.95	–
SO_3	3.80	0.19
K_2O	1.10	1.11
Na_2O	0.20	2.75
Loss on ignition	2.10	0.21
Physical properties		
Specific gravity	3.15	2.18
Retained on 45 μm (0.002 in.) (%)	12.9	9.6
Water requirement (%)	–	93.4

Table 2
Mixture properties of ECC.

Mix ID.	Ingredients (kg/m^3)						FA/C	Compressive strength (MPa)			
	C	FA	Water	PVA	Sand	SP		w/o fiber		With fiber	
								14-day	28-day	14-day	28-day
ECC1	558	669	326	26	446	2.3	1.2	36.1	60.3	39.2	62.5
ECC2	375	823	318	26	435	2.0	2.2	25.8	52.4	27.7	54.1

Table 3
Uniaxial tensile properties of ECC specimens.

Age	Tensile Strain (%)		Tensile Strength (MPa)		Residual Crack Width (μm)	
	14-day	28-day	14-day	28-day	14-day	28-day
ECC1	2.91 ± 0.22	2.73 ± 0.24	4.63 ± 0.48	5.14 ± 0.31	~60	~48
ECC2	3.24 ± 0.14	3.02 ± 0.19	4.17 ± 0.36	4.82 ± 0.27	~40	~30

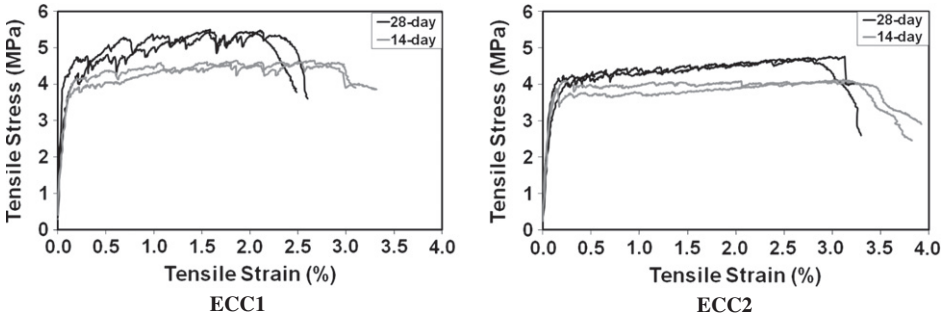

Fig. 1. Typical tensile stress–strain response of standard ECC mixtures.

capacity [5]. On the other hand, the increase in the FA content slightly reduced the tensile strength, but remains above 4.0 MPa at all ages. Table 3 gives also the effect of FA content on the residual crack width at different ages. It was found that the crack width reduces significantly as FA content increases at all ages. The reason for this is likely associated with the higher fiber/matrix interface frictional bond with the increase of FA content [5].

2.2. Specimen preparation and testing for frost resistance and air-void characterization

From each mixture, eight 400 × 100 × 75 mm prisms were prepared for the freezing and thawing test and determination of air-void characteristics. The air content of the freshly mixed ECC and ECC matrix mixtures were also measured in accordance with ASTM C231 [12]. All specimens were cast in one layer without compaction, demolded at the age of 24 h, and moist cured at 23 ± 2 °C for 13 days.

Fourteen days after casting, the beam specimens were moved into the freeze–thaw chamber in accordance with ASTM C666 Procedure A [13], consisting of 18 chambers in which specimens were completely surrounded by water, and subjected to between five and six freezing and thawing cycles in a 24-h period, with a thermocouple embedded in the center of one prism in each cabinet to insure proper cycle control. The freeze–thaw cycle consisted of alternately lowering the temperature of the specimens from 4 to −18 °C and raising it from −18 to 4 °C in 4–5 h. The average flexural parameters (ultimate deflection and flexural strength) of the specimens were obtained by testing four companion samples just prior to the freezing and thawing cycles at the age of 14 days, and the result was used as the basis for determining the preloading flexural performance (control). Specimens were removed for tests when they were in a thawed condition at each 30 cycle intervals. The masses and pulse velocities were measured. Before returning specimens to the freeze–thaw apparatus in a random order, containers were cleaned out and fresh water was added. The number of cycles to failure for the specimens was also monitored. At the end of 300 freeze–thaw cycles, surviving specimens were tested under four-point bending load with a span length of 355 mm and a height of 75 mm to determine their residual flexural performances, and their load-deflection curves were recorded. Four-point bending test was performed under displacement control at a loading rate of 0.005 mm/s on a closed-loop controlled servo-hydraulic material test system. The top surface was polished to obtain a perfect contact with the fulcrum points. Freeze–thaw resistance was determined in triplicate on all ECC mixtures with and without fiber.

The air-void content and spacing factor of hardened ECC and matrix (ECC without fiber) mixtures were determined by modified point count method according to ASTM C457 [14]. Mercury intrusion porosimetry analysis (MIP) was also used to characterize the pore size distribution of the virgin and frost deteriorated ECC and ECC matrix mixtures. An instrument capable of producing pressures up to 414 MPa and assuming a contact angle of 130° was used for pore size distribution analysis by the mercury intrusion method. Specimens were dried to constant weight at 50 °C prior to testing. All tests included at least two identical specimens tested at the same time.

3. Experimental results and discussions

3.1. Air-void characterization

Air-void parameters of the hardened ECC and ECC matrix mixtures determined by modified point count method according to ASTM C457, are shown in Table 4, along with the air content

measured in the fresh state according to ASTM C231. For each mixture, only the average values obtained from two specimens are shown in the table. It is important to note that concretes containing HRWR often tend to have air voids that are larger than those in conventional concrete [15]. Such air void systems tend to be less stable and have larger spacing factors. Since the similar dosages of HRWR is used in the production of ECC matrix and ECC mixtures, HRWR admixture cannot be a factor responsible for the great differences in the frost durability of ECC and ECC matrix, which will be discussed in the next section.

The frost durability of concrete has a close relationship with its air-void parameters. As seen in Table 4, although no air entraining admixture was added to the ECC and ECC matrix mixtures, the air contents of these mixtures in the fresh state, as measured by ASTM C231, gave values between 6% and 7%, and in the hardened state, as measured by ASTM C457, gave values of more than 7% for all mixtures. This amount of air content is adequate for freeze–thaw durability [16]. The apparently high air content in these mixtures may have resulted from the absence of coarse aggregate and the higher viscosity of the ECC matrix in the fresh state [17]; the fine particles and high viscosity tend to prevent some of the air bubbles from rising to the surface during placing operations. Moreover, the air contents measured during the fresh state of the ECC mixtures show that this phenomenon is amplified after the addition of PVA fiber to the mixtures (Table 4). When PVA fiber is added to the ECC matrixes, it increases the viscosity of the fresh ECC mixtures compared to the ECC matrix [11], which further increases the amount of entrapped air voids inside the matrix. Another reason of increased the amount of air voids with the addition of PVA fibers may be attributed to the proprietary hydrophobic oiling agent of 1.2% by mass coated on the surface of the PVA fibers to tailor the interfacial properties between fiber and matrix for strain-hardening performance. The proprietary coating chemical used on the surface of fibers may also entrain very small air bubbles, thus enhancing the freeze–thaw durability of ECC mixtures. Further study will be conducted to understand the reason of increase in air content with PVA fiber addition, which is beyond the scope of the present paper.

Hardened air content of 8.2% and 8.9%, spacing factors of 0.241 and 0.149 mm and specific surfaces of 25.6 and 39.5 mm^{-1} were determined for ECC1 and ECC2 mixtures, respectively. Though the spacing factor values of ECC1 (0.241 mm) slightly exceed the generally accepted value of 0.200 mm for good freeze–thaw durability, this lack of an apparently ideal air-void system has not adversely affected the frost durability of ECC1, as indicated in the following section. From Table 4, it can be observed that the increase in the FA content in hardened ECC mixtures leads to a significant decrease in spacing factor. Almost similar air content together with a lower spacing factor implies that the average bubble size is decreased with the increase in the FA content. This is more likely due to the fact that an increase in FA content results in an increase in volume of paste due to its lower density and pore refinement of FA (transformation of a system containing larger pores into smaller pores). As in the non-air entrained mortar incorporating silica fume postulated by Feldman [18], FA in the ECC may also create its own micro air void network around fine aggregate particles as a result of the consumption of the calcium hydroxide (CH) in pozzolanic reaction, leaving voids. On the other hand, since the pozzolanic reaction involving FA is slower than regular cement hydration, there is a significant amount of unhydrated FA in the high-volume FA ECC after short time curing (14 days in this study), and therefore the addition of FA in ECC still leads to higher porosity in the matrix.

Table 4
Air-void parameters of ECC mixtures.

	ECC1 (M45)		ECC2	
	With PVA	w/o PVA	With PVA	w/o PVA
Fresh air content (%)	7.3	5.9	7.1	6.2
Hardened air content (%)	8.2	7.3	8.9	7.9
Specific surface (mm^{-1})[a]	25.6	53.0	39.5	91.3
Spacing factor (mm)[a]	0.241	0.129	0.149	0.069
Average chord length (mm)	0.156	0.125	0.101	0.117

[a] For freeze/thaw resistant concrete, the American Concrete Institute (ACI) recommends that [15]: Min. specific surface = 24 mm^{-1}, and Maximum spacing factor = 0.2 mm.

Except for the spacing factor value of ECC1, air-void parameters of all hardened ECC and ECC matrix mixtures conform to specifications ASTM C 457 for frost durability. In the case of hardened ECC mixtures, it is interesting to note that the addition of the PVA fiber can result in a significant increase in spacing factor (see Table 4). Moreover, specific surface of the air void system is significantly higher for both ECC matrixes (w/o PVA fiber) when compared with ECC mixtures, which indirectly implies that the average bubble size is smaller in ECC matrixes. This is likely due to the fact that the randomly distributed PVA fibers form a network that provides a path for the air bubbles to coalesce, thus creating large entrapped air voids instead of finely distributed air voids (Fig. 2) [10]. Other than this difference, the air-void distributions are similar in ECC and ECC matrix mixtures. This is not in agreement with the results of the frost durability study described in Section 3.2 which concludes that ECC and ECC matrix mixtures essentially behave differently when subjected to freezing and thawing cycles.

The microstructural characterization in terms of pore size distributions for samples obtained from the same depth below the surface of beam specimen is examined before and after exposure to 300 freeze and thaw cycles by using MIP. MIP is a well-developed technique that can provide information about pore structure, including the porosity, average pore diameter and pore size distribution of ECC. Typical pore size distribution curves are shown in Fig. 3 for the ECC and ECC matrix (w/o fiber) samples before and after frost deterioration. Since the curves obtained from duplicate specimens are similar, only one curve is given in Fig. 3 for each mixture. MIP test results for the ECC and ECC matrix specimens prepared at w/cm ratio of 0.27 before frost deterioration are shown in Table 5. Since matrix (ECC w/o fiber) specimens had severely deteriorated as a result of frost deterioration, microstructural studies after frost deterioration were not performed for ECC matrix specimens.

As seen from Table 5, the ECC mixtures exhibited a higher total porosity when compared with the corresponding ECC matrixes. However previous studies have shown that the total porosity is not a good indicator of frost durability, since very small gel pores would not contribute to increased frost durability [19]. The radius and size distribution of pores determine the freezing point of pore solution and the amount of ice formed in pores [20]. According to current literature, while a uniform relationship between frost resistance and pore size distribution obtained by MIP technique has not been found, in general, a larger volume of coarse pores (greater than approximately 0.30 μm diameter [21–25]) results in higher freeze–thaw resistance.

Results for 28 day cured specimens for pore size ranges of larger than 2 μm and between 0.30 and 2 μm are presented in Table 5. The pore volumes for 28 day cured specimens in these sizes generally increase considerably with PVA fiber addition, with the total volume (including both pore size ranges) for the 28 day specimen being 5.0% and 5.2% for ECC1 and ECC2, and 0.7% and 1.4% for ECC1 matrix and ECC2 matrix, respectively. The significant and unique increase of pore volume larger than 0.30 μm diameter suggests that pores of this size may be responsible for the increased frost resistance of non-air-entrained ECC mixtures, which is

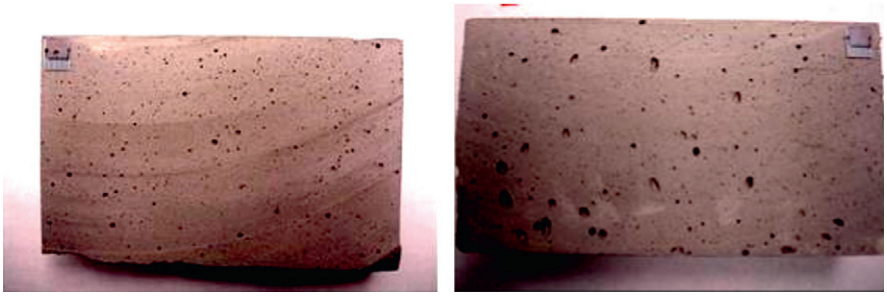

ECC matrix (w/o PVA fiber) ECC (with PVA fiber)

Fig. 2. Typical air voids in a non-air-entrained ECC specimens (without and with fiber).

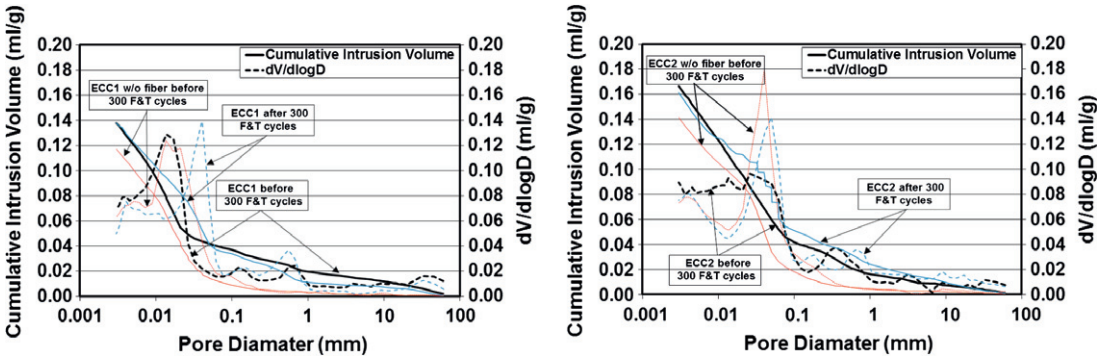

Fig. 3. Comparison of pore size distribution of ECC mixtures and their matrixes with different FA/C ratios before F&T cycles.

Table 5
Pore size distribution of ECC mixtures before and after frost deterioration.

Specimen	ECC1 (M45)				ECC2			
	Before F&T		After F&T		Before F&T		After F&T	
	With PVA	w/o PVA	With PVA	w/o PVA	With PVA	w/o PVA	With PVA	w/o PVA
Volume of pores > 2	2.9	0.3	1.7	–	2.2	0.6	3.2	–
0.30 < Volume of pores < 2	2.1	0.4	2.6	–	3.0	0.8	3.3	–
Volume of pores < 0.30	18.7	18.5	19.6	–	22.0	23.0	20.8	–
Total intruded porosity	23.7	19.2	23.9	–	27.2	24.4	27.3	–

contradictory to the present view of the mechanism of protection by air entrainment.

The MIP curves and Table 5 also show that the total intruded porosity increases with the increase of FA content. Comparing the total pore volumes of ECC and matrix mixtures with FA/C ratios of 1.2 and 2.2 for the pore size range less than 0.30 μm, ECC mixture with FA/C ratio of 2.2 (ECC2) is found to have almost 5% higher pore volume. This might be attributed to the slower pozzolanic reaction involving FA than cement hydration; after short time curing, there remains a significant amount of unhydrated FA in ECC2 mixture (Fig. 4). After 300 freezing and thawing cycles, as seen from Table 5 and Fig. 3, the total intruded porosity of ECC mixtures does not appear to be affected. This result is consistent with the results of the residual physical/mechanical performances of ECC mixtures reported in Section 3.2.

3.2. Freezing and Thawing Resistance

3.2.1. Mass loss and pulse-velocity measurements

The addition of FA and micro-PVA fiber on freeze–thaw durability of ECC and ECC matrix mixtures were assessed by the calculation of mass loss, which is a measure of scaling. To measure the internal damage caused by freezing and thawing cycles, the changes in pulse velocity through a prism were also measured. Normally, ASTM C666 specifies the use of the resonant frequency method, not the pulse velocity method. However, previous studies have shown that pulse velocity test method can also be used to measure the deterioration of specimens during freezing and thawing cycles [26]. The travel time for the ultrasonic pulse velocity was measured in the longitudinal, since the transverse measurement has a shorter time travel, which results in less accurate reading than longitudinal measurement due to resolution of time measurement [27].

The freeze–thaw durability test results are summarized in Table 6. Fig. 5 shows the reduction in the average relative pulse velocity (V_i/V_0) and relative mass change (M_i/M_0) with the number of freezing and thawing cycles. V_i and M_i are the pulse velocity and mass, respectively, after a specific number of freezing and thawing cycles, and V_0 and M_0 are initial pulse velocity and mass, respectively, prior to any freezing and thawing cycles. As seen in Fig. 5, the mass and pulse velocity losses of ECC matrixes increase with the number of freeze–thaw cycles and FA content. This trend is similar to but

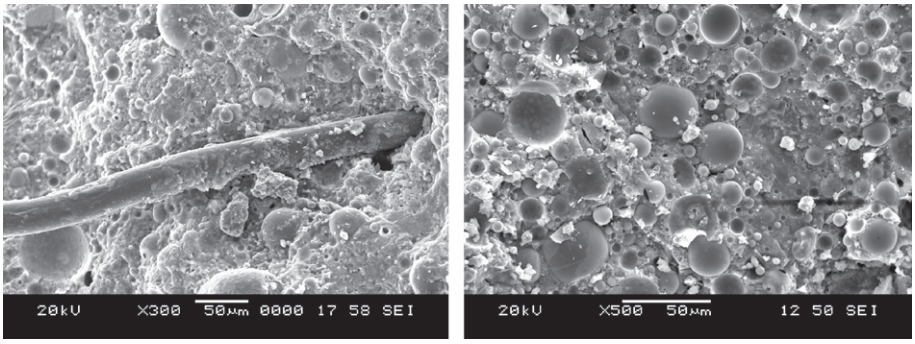

Fig. 4. SEM micrograph of ECC mixtures at the age of 28 days.

Table 6
Freezing and thawing resistance of ECC and ECC matrix.

	ECC1 (M45)		ECC2 (M45)	
	w/o PVA	With PVA	w/o PVA	With PVA
# of cycles completed	210	300	60	300
Change in mass (%)	−7.3	−1.3	−10.7	−8.0
Pulse velocity change (%)	−30.9	−2.2	−32.6	−4.7

less severe than that for the corresponding ECC mixtures, as shown in Fig. 5. Fig. 5 indicates that a higher amount of air content and significantly lower spacing factor did not benefit ECC matrix mixtures in meeting the minimum durability factor requirement of ASTM C666. After 60 cycles, the ECC2 matrix specimens and after 210 cycles, the ECC1 matrix specimens had severely deteriorated, requiring removal from the freeze–thaw machine (typical normal strength, non-air-entrained concrete prisms usually fail in 60–95 cycles in this apparatus). The deterioration of typical specimens of ECC1 matrix specimens after 210 cycles and ECC2 matrix specimens after 60 cycles is shown in Fig. 6. Fig. 6 (a and b) shows also that ECC2 matrix specimen has totally disintegrated as a result of accelerated freeze–thaw cycles. Different from ECC2 matrix specimens, distress in ECC1 without PVA fiber is limited mostly to extremities of the specimen. This may due to the lower maturity – lower compressive strength of ECC2 specimens (because of its higher FA content) at the time of testing.

The effect of micro-PVA fiber on the average relative mass loss and ultrasonic pulse velocity of ECC mixtures is presented in Fig. 5. Fig. 5 demonstrates that, both ECC mixtures showed excellent performance when exposed to freezing and thawing cycles, even after 300 cycles. The addition of PVA fiber to ECC matrixes improved the freeze–thaw resistance considerably; and, the improvement was more than enough to make the mixture acceptable according to ASTM C666, Procedure A. A maximum of 1.3% and 2.2%, and 8.0% and 4.7% mass and pulse velocity losses, respectively, were measured for the ECC1 and ECC2 specimens, respectively. Note that at the end of 300 cycles, ECC2 has a lower relative pulse velocity and mass loss values than ECC1 at the same number of freeze–thaw cycles though ECC2 had a higher hardened air content and significantly lower spacing factor than ECC1. Therefore, it is not possible on this figure to determine the critical spacing factor for

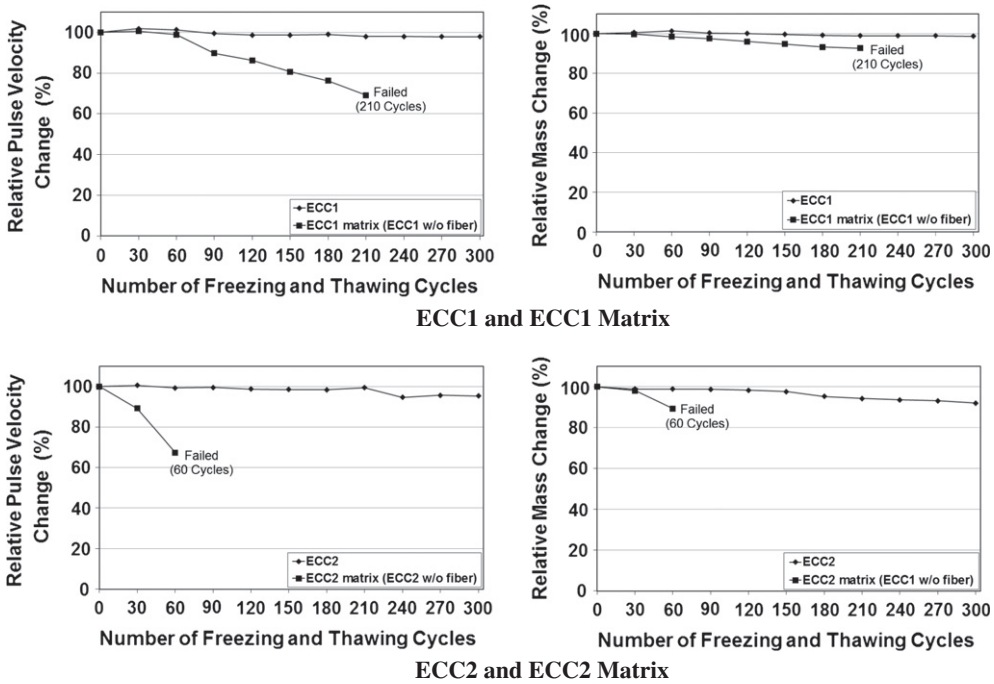

Fig. 5. Relative pulse velocity and mass loss changes as a function of number of freezing and thawing cycles.

(a) ECC1 matrix (ECC1 w/o fiber) after 210 freezing and thawing cycles

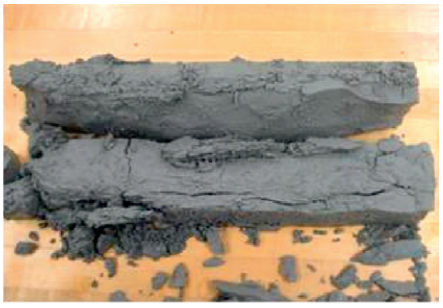

(b) ECC2 matrix (ECC2 w/o fiber) after 60 freezing and thawing cycles

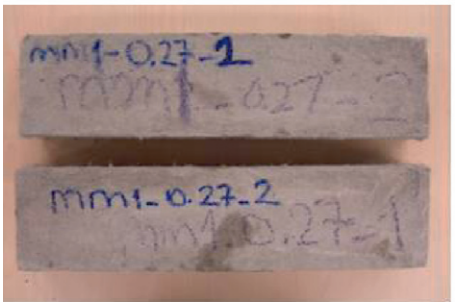

(c) ECC1 after 300 freezing and thawing cycles

(d) ECC2 after 300 freezing and thawing cycles

Fig. 6. Specimens surface appearance after freeze–thaw cycles.

ECC with high volume FA, since they were both found to be frost resistant.

In general, the ECC specimens exhibited some surface scaling at the conclusion of the freeze–thaw cycling. Reduced surface scaling was observed on the ECC1 specimens compared to ECC2 specimens. This was probably due to the greater maturity (higher compressive strength at the time of testing; see Table 2) of the former test specimens because of lower FA content. The scaling was, however, clearly confined to the surface layers of the test specimens, and had no effect on the integrity and mechanical properties of the ECC mass (see Section 3.2.2 and Fig. 6 c and d).

There are a number of possible explanations for the excellent performance of these non-air entrained ECC samples. A proper air-void system is needed in normal concrete to avoid internal cracking due to freezing and thawing cycles. As discussed in the preceding section, the pore size distributions of matrix mixtures are much finer (i.e. fewer coarse pores) than ECC mixtures. To make a general conclusion regarding the influence of pore size distribution on frost resistance, large pores are beneficial to frost resistance of concrete, whereas small and intermediate pores are detrimental (see Section 3.1).

Another possible reason for ECC's excellent frost resistance can be attributed to its high ductility under tensile loadings (see Section 3.2.2). It is well known that upon freezing, water in capillary pores expands. If the required volume is greater than the space available, the pressure build-up could reach the tensile strength of the material, resulting in local micro-crack formation, brittle rupture and scaling. Therefore, the high tensile strength – and particularly fracture resistance in ECC – could lead to its higher frost resistant characteristic. The influence of micro-fiber addition on frost resistance of conventional concrete has also been examined by other researchers [10,28,29], and is in agreement with what is found in this study. When PVA fiber is incorporated into ECC matrix, both the pressure-releasing effect (due to larger pore size (see Section 3.1 above)) and the crack-resisting effect contribute to the ability to resist disintegration during freezing and thawing cycles.

3.2.2. Residual flexural performance

A summary of the modulus of rupture test results before and after freezing and thawing deterioration is given in Table 7. Each reading represents the average value of three to four specimens. Typical flexural stress – mid-span beam deflection curves of ECC and ECC matrix (without fiber) specimens before and after freezing and thawing deterioration are shown in Fig. 7. The flexural strength in Table 7 is defined as the ultimate stress on the flexural stress-mid-span beam deflection curve, and its corresponding deflection is the ultimate deflection.

As seen in Table 7, the average flexural strengths were 11.44 and 4.42 MPa for ECC1 and ECC1 matrix, and 9.19 and 3.47 MPa for ECC2 and ECC2 matrix, respectively, just prior to freezing and thawing cycles. The ECC mixtures for both FA/C ratios show more than two times higher ultimate flexural strength than that of ECC matrix mixtures. This may be attributed to the fact that micro fibers inhibit the localization of microcracks into macrocracks and consequently, the flexural strength of the ECC matrix increases with the formation of multiple microcracks during inelastic deformation. In all of the ECC mixtures with/without freezing and thawing deterioration, prismatic specimens showed multiple cracking behaviors with small crack spacing and tight crack widths (less than 70 μm). The first crack started inside the mid-span at the tensile face. The flexural stress increased at a slower rate, along with the development of multiple cracks with small crack spacing and tight crack widths. Microcracks developed from the first cracking point and spread out in the mid-span of the flexural beam, as shown in Fig. 8. Bending failure in the ECC occurred when the fiber-bridging strength at one of the microcracks was reached; resulting in localized deformation once the modulus of rupture was approached. On the other hand, because of their low tensile properties and brittle nature, the ECC matrix beam specimens

Table 7
Flexural properties of ECC prisms before and after 300 freeze–thaw cycles.

Specimen type			Ultimate deflection (mm)	Flexural strength (MPa)	Crack width (μm)
Cured 14 days in lime-saturated water	ECC1	w/o fiber	0.68 [0.24][a]	4.42 [0.79]	–
		With fiber	5.23 [0.16]	11.44 [0.54]	~61 [~13]
	ECC2	w/o fiber	0.82 [0.11]	3.47 [0.36]	–
		With fiber	6.01[0.36]	9.19 [0.54]	~44 [~10]
Subjected to 300 F&T cycles	ECC1	With fiber	4.91 [0.40] (93.9)[b]	9.70 [0.19] (84.8)	~70 [~28]
	ECC2	With fiber	4.88 [0.27] (81.2)	6.93 [0.65] (74.3)	~78 [~19]

[a] Numbers in brackets are standard deviations.
[b] Numbers in parentheses are residual flexural properties (deflection or strength), in percentage.

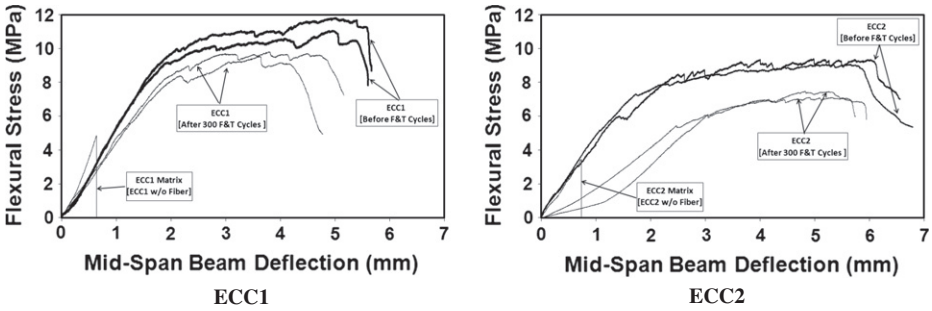

Fig. 7. Effect of freezing and thawing cycles on flexural behavior of ECC mixtures.

failed catastrophically with a single crack under the four-point bending test.

The complete flexural stress – mid-span deflection curves for ECC specimens before cycling and after 300 freezing and thawing cycles are shown in Fig. 7. The effect of 300 cycles of freezing and thawing was evident on the stress–strain curve, especially for ECC2 specimens. Compared to control specimens cured in laboratory air, the ascending portion of the flexural stress – deflection diagram indicated less stiffness (the slope of the load-deflection curve) with a smaller first crack and maximum stress, and smaller inelastic deformation. The typical flexural stress-mid-span beam deflection curves of ECC specimens after frost deterioration show that the influence of 300 freezing and thawing cycles on the flexural stress-mid-span deflection curves is fairly minor especially for ECC1 specimens. The ultimate mid-span beam deflection capacity of ECC specimens, which reflects material ductility, exposed to frost deterioration is 4.91 mm for ECC1 (93.9% of its original ductility) and 4.88 mm for ECC2 (81.2% of its original ductility). The 4.0 mm deformation is nearly equivalent to 2% strain on the tensile face of the beam [30]. Increasing levels of FA lead to higher reductions in the tensile strain capacity compared with standard ECC mixture (ECC1, M45). This result is consistent with the earlier results of mass and pulse velocity losses of ECC specimens after 300 freezing and thawing cycles (Fig. 5). The reduction in flexural performance of ECC mixtures may be attributed to the effects of damage on the fiber/matrix interface and matrix micro-cracking. Despite a reduction in stiffness, ductility and flexural strength, both of the ECC mixtures after 300 cycles of freezing and thawing exposure are found to retain ductility and flexural strength significantly more than that of normal concrete and FRC with no environmental exposure. For this reason, it is expected that the ECC mixtures investigated in this study are suitable for long-term application under severe freeze–thaw environments if the structure is designed based on long term mechanical properties.

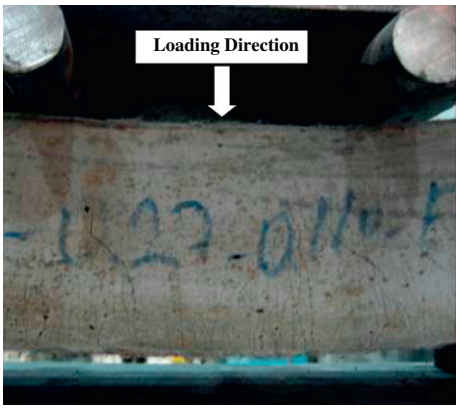

Fig. 8. Typical multiple crack pattern of ECC beam specimen during flexure load applications.

It should also be noted that the residual ultimate flexural load-deflection curves of frost deteriorated ECC beams obtained following induced accelerated freeze–thaw cycling (up to six freezing and thawing cycles were achieved in a 24-h period) provide a conservative estimate of their residual flexural properties in actual structures. These accelerated deterioration periods are equivalent to a time span of many years in real structures, even those located in regions with harsh winters. This difference in accelerated and normal frost deterioration periods should have a significant influence on the residual flexural properties of ECC because in the long term, deterioration in ECC as a result of freezing and thawing cycles can easily be closed due to a self-healing process [7,9,31–34]. By neglecting this self-healing capability of ECC, thus, a conservative estimation for the flexural performance of the material is presented.

Table 7 also shows the residual crack width of ECC mixtures at different ages. The term "residual crack width" indicates that crack width was measured from the unloaded specimen after the four-point flexural test by using a portable microscope with an accuracy of 5 μm. Both frost-deteriorated and virgin ECC specimens revealed saturated multiple cracking (Fig. 8) with crack width at ultimate flexural load limited to below 100 μm. Crack width control is of primary importance for many reinforced concrete applications since it is believed that there is a close relationship between mean or maximum crack widths and the durability of the structure.

Moreover, the lower magnitude of the crack width is expected to promote self-healing behavior, and thus the transport properties in cracked composites [31–34]. In terms of permeability and diffusion, crack width less than 100 μm generally behaves like sound concrete [31,35]. Based on experimental results, Şahmaran et al. [31], Evardsen [36], and Reinhardt and Jooss [37] proposed that cracks with a width below 100 μm can be easily closed by a self-healing process. Consequently, in the serviceability limit state, a mean or maximum crack width less than about 0.1 mm is usually prescribed.

4. Conclusions

The objective of this research is to assess the effect of fly ash (FA) and micro poly-vinyl-alcohol (PVA) fibers on the microstructure and frost durability of the non-air-entrained Engineered Cementitious Composites (ECC). ECC mixtures with two different contents of FA as a replacement of cement (55% and 70% by weight of total cementitious material) were prepared. To find out the effect of PVA fibers on frost durability of ECC, matrix mixtures of same composition but without PVA fiber were also produced and tested for the frost resistance. The frost resistance assessed by alternate freezing and thawing cycles in accordance with ASTM C666 Procedure A, air-void parameters determined by the modified point count method (ASTM C452), and the pore size distribution obtained by mercury intrusion porosimetry technique were compared with ECC matrix (w/o PVA fiber).

Although the control ECC matrix mixtures specimens rapidly failed in freezing and thawing cycles (after 60 cycles, the ECC2 matrix (FA/C = 2.2) specimens and after 210 cycles, the ECC1 matrix (FA/C = 1.2)), both ECC mixtures showed excellent performance when exposed to freezing and thawing cycles, even after 300 cycles. The addition of PVA fiber to ECC matrixes improved the freeze–thaw resistance considerably; and, the improvement was more than enough to make the mixture acceptable according to ASTM C666, Procedure A. Apart from the slight reduction in ultimate flexural strength and ductility, the test results presented in this study confirm that ECC provides excellent frost protection compared to ECC matrix. Increasing levels of FA lead to higher reductions in the mechanical performances compared with standard ECC mixture (ECC1, M45) due to the lower maturity – lower compressive strength at the time of testing. Apart from the slight reductions in ductility and strength capacities and higher residual crack width, the results presented in this study largely confirm the durability performance of ECC material incorporating high volume of FA under frost exposure. The presence of micro PVA fibers critically contributes to the higher crack resistance and larger pore volume, and resulting pressure-releasing effects under freeze–thaw conditions. In addition to superior ductility and high tensile strength properties, a large pore volume (>∼0.3 μm) in the presence of a PVA fiber is assumed to be responsible for the improved frost resistance of ECC mixtures. Recall that this high frost durability was achieved without deliberate air entrainment into the ECC. Normally, concrete durability remains very sensitive to the amount of air entrainment, air-void parameters, strength and maturity of concrete. Since this sensitivity can be overcome through an ECC material solution even with high volume fly ash and without air-entraining admixture, the ultimate result will be overall improved structural durability.

Acknowledgments

The authors gratefully acknowledge the financial assistance of the Scientific and Technical Research Council (TUBITAK) of Turkey provided under Project: MAG-108M495, Gaziantep University Scientific Research Centre provided under Project: MF.10.09 and Higher Education Council of Turkey (YOK).

References

[1] Li VC. Engineered cementitious composites – tailored composites through micromechanical modeling. In: Banthia N, Bentur A, Mufti A, editors. Fiber reinforced concrete: present and the future. Montreal: Canadian Society for Civil Engineering; 1997. p. 64–97.
[2] Li VC. On engineered cementitious composites (ECC) – a review of the material and its applications. J Adv Concr Technol 2003;1(3):215–30.
[3] Li VC, Wang S, Wu C. Tensile strain-hardening behavior of PVA-ECC. ACI Mater J 2001;98(6):483–92.
[4] ECC Applications. <http://ace-mrl.engin.umich.edu/NewFiles/eccapp.html>. [07.11].
[5] Wang S, Li VC. Engineered cementitious composites with high-volume fly ash. ACI Mater J 2007;104(3):233–41.
[6] Yang EH, Yang Y, Li VC. Use of high volumes of fly ash to improve ECC mechanical properties and material greenness. ACI Mater J 2007;104(6):620–8.
[7] Şahmaran M, Li VC. Durability properties of micro-cracked ECC containing high volumes fly ash. Cem Concr Res 2009;39(11):1033–43.
[8] Lepech MD, Li VC. Long term durability performance of engineered cementitious composites. Int J Restor Build Monument 2006;12(2):119–32.
[9] Şahmaran M, Li VC. De-icing salt scaling resistance of mechanically loaded engineered cementitious composites. Cem Concr Res 2007;37(7):1035–46.
[10] Şahmaran M, Lachemi M, Li VC. Assessing the durability of engineered cementitious composites under freezing and thawing cycles. J ASTM Int 2009;6(7):1–13.
[11] Yang E, Şahmaran M, Yang Y, Li VC. Rheological control in the production of engineered cementitious composites. ACI Mater J 2009;106(4):357–66.
[12] ASTM C231-97. Standard test method for air content of freshly mixed concrete by the pressure method. Annual Book of ASTM Standards. West Conshohocken (PA): ASTM; 2002.
[13] ASTM C666-97. Standard test method for resistance of concrete to rapid freezing and thawing. Annual Book of ASTM Standards. West Conshohocken (PA): ASTM; 2002.
[14] ASTM C457-98. Standard test method for microscopical determination of parameters of the air-void system in hardened concrete. Annual Book of ASTM Standards. West Conshohocken (PA): ASTM; 2002.
[15] Siebel E. Air-void characteristics and freezing and thawing resistance of superplasticized air-entrained concrete with high workability. ACI Special Publication 1989;119:297–320.
[16] Pigeon M, Pleau R. Durability of concrete in cold climates. London: Chapman & Hall; 1995.
[17] Powers TC. Frost resistant concrete. J PCA Res Dev Lab 1964;6:19.
[18] Feldman RF. Influence of condensed silica fume and sand/sement ratio on pore structure and frost resistance of portland cement mortars. Fly ash, Silica Fume, Slag and Natural Pozzolans in Concrete, SP-91. American Concrete Institute; 1986. p. 973–89.
[19] Hooton RD. Influence of silica fume replacement of cement on physical properties and resistance to sulfate attack, freezing and thawing, and alkali–silica reactivity. ACI Mater J 1993;90(2):143–51.
[20] Cai H, Liu X. Freeze–thaw durability of concrete: ice formation process in pores. Cem Concr Res 1998;28(9):1281–7.
[21] Litvan GG. Air entrainment in the presence of superplasticizers. ACI J Proc 1983;80(4):326–31.
[22] Koh Y, Kamada E. The influence of pore structure of concrete made with absorptive aggregates on the frost durability of concrete. In: Proceedings RILEM/IUPAC international symposium on pore structure and properties of materials, Prague, Artia, vol. 11; 1973. p. F45–62.
[23] Cebeci OZ. Pore structure of air-entrained hardened cement paste. Cem Concr Res 1981;11(2):257–65.
[24] Litvan GG, Sereda PJ. Particulate admixture for enhanced freeze–thaw resistance of concrete. Cem Concr Res 1977;8(1):53–60.
[25] Lange H, Modry S. Determination of the frost resistance of limestone aggregates in the light of porosity investigation. In: Proceedings, Rilem Symposium on Durability of Concrete. Prague: Building Research Institute; 1969. p. B129–68.
[26] Cohen MD, Zhou Y, Dolch WL. Non-air-entrained high strength concrete—is it frost resistant? ACI Mater J 1992;89(4):406–15.
[27] Marzouk H, Jiang D. Effects of freezing and thawing on the tension properties of high-strength concrete. ACI Mater J 1994;91(6):577–86.
[28] Pigeon M, Azzabi M, Pleau R. Can microfibers prevent frost damage? Cem Concr Res 1996;26(8):1163–70.
[29] Deja J. Freezing and de-icing salt resistance of blast furnace slag concretes. Cem Concr Compos 2003;25(3):357–61.
[30] Qian S, Li VC. Simplified inverse method for determining the tensile properties of strain hardening cementitious composites (SHCC). J Adv Concr Technol 2008;6(2):353–63.
[31] Şahmaran M, Li VC, Li M. Transport properties of engineered cementitious composites under chloride exposure. ACI Mater J 2007;104(6):604–11.
[32] Şahmaran M, Li VC. Influence of microcracking on water absorption and sorptivity of ECC. Mater Struct 2009;42(7):1015–23.

[33] Lepech MD, Li VC. Water permeability of cracked cementitious composites. Paper 4539 of Compendium of Papers CD ROM. Turin: ICF 11; 2005.
[34] Yang Y, Lepech MD, Li VC. Self-healing of ECC under cyclic wetting and drying. in: Proceedings of International Workshop on Durability of Reinforced Concrete under Combined Mechanical and Climatic Loads. Qingdao; 2005. p. 231–42.
[35] Wang K, Jansen D, Shah S, Karr A. Permeability study of cracked concrete. Cem Concr Res 1997;27(3):381–93.
[36] Evardsen C. Water permeability and autogenous healing of cracks in concrete. ACI Mater J 1999;96(4):448–54.
[37] Reinhardt HW, Joos M. Permeability and self-healing of cracked concrete as a function of temperature and crack width. Cem Concr Res 2003;33(7):981–5.